provide a conclusive demonstration of the principle of the enhancement of nonlinear optical response through the supramolecular engineering of polymers. It is expected that considerably larger enhancement can be observed in structures with better alignment of chromophores, such as certain biopolymers and derivatives of helical poly(triphenylmethylmethacrylate)s (*16*).

REFERENCES AND NOTES

1. See, for example, P. N. Prasad and D. J. Williams, *Introduction to Nonlinear Optical Effects in Molecules and Polymers* (Wiley, New York, 1991).
2. J.-M. Lehn, *Supramolecular Chemistry* (VCH, Weinheim, Germany, 1995).
3. K. Clays *et al.*, *Science* **262**, 1419 (1993).
4. E. Kelderman *et al.*, *Adv. Mater.* **5**, 925 (1993).
5. C. T. O'Konski, K. Yoshioka, W. H. Orttung, *J. Phys. Chem.* **63**, 1558 (1959).
6. R. J. M. Nolte, A. J. M. van Beijnen, W. Drenth, *J. Am. Chem. Soc.* **96**, 5932 (1974); R. J. M. Nolte, *Chem. Soc. Rev.* **23**, 11 (1994).
7. M. N. Teerenstra *et al.*, *Thin Solid Films* **248**, 110 (1994).
8. R. J. M. Nolte and W. Drenth, in *New Methods for Polymer Synthesis*, W. J. Mijs, Ed. (Plenum, New York, 1992), pp. 273–310. For a discussion of the structure of poly(isocyanide)s, see also M. M. Green, R. A. Gross, F. C. Schilling, K. Zero, C. Crosby III, *Macromolecules* **21**, 1839 (1988); C. Kollmar and R. Hoffman, *J. Am. Chem. Soc.* **112**, 8230 (1990).
9. C. J. M. Huige, A. M. F. Hezemans, R. J. M. Nolte, W. Drenth, *Recl. Trav. Chim. Pays-Bas* **112**, 33 (1993).
10. R. W. Terhune, P. D. Maker, C. M. Savage, *Phys. Rev. Lett.* **14**, 681 (1965).
11. K. Clays and A. Persoons, *ibid.* **66**, 2980 (1991); *Rev. Sci. Instrum.* **63**, 3285 (1992).
12. T. Verbiest, E. Hendrickx, A. Persoons, K. Clays, in *Nonlinear Optical Properties of Organic Materials V*, D. J. Williams, Ed. [*Proc. SPIE* **1775**, 206 (1993)].
13. G. S'heeren, L. Derhaeg, T. Verbiest, C. Samyn, A. Persoons, *Makromol. Chem., Makromol. Symp.* **69**, 193 (1993).
14. R. S. Becker, *Theory and Interpretation of Fluorescence and Phosphorescence* (Wiley, New York, 1969), chap. 16.
15. R. Bersohn, Y.-H. Pao, H. L. Frisch, *J. Chem. Phys.* **45**, 3184 (1966).
16. T. Nakano, Y. Okamoto, K. Hatada, *J. Am. Chem. Soc.* **114**, 1318 (1992).
17. M. N. Teerenstra *et al.*, in preparation.

18. Supported by grants from the government of Belgium (IUAP-16), the Belgian National Science Foundation (FKFO 9.0011.92), and the University of Leuven (GOA95/1) (to M.K., T.V., C.B., K.C., and A.P.) and from the Dutch Ministry of Economical Affairs (IOP-PCBP 105) (to M.N.T., A.J.S., and R.J.M.N.). M.K. is a research fellow of the University of Leuven; T.V. is a postdoctoral researcher and K.C. is a senior research associate of the Belgian National Fund for Scientific Research (NFWO).

11 July 1995; accepted 11 September 1995

Carbon Dioxide and Oxygen Isotope Anomalies in the Mesosphere and Stratosphere

Mark H. Thiemens,* Teresa Jackson, Edward C. Zipf, Peter W. Erdman, Cornel van Egmond

Isotopic ($\delta^{17}O$ and $\delta^{18}O$) measurements of stratospheric and mesospheric carbon dioxide (CO_2) and oxygen (O_2), along with trace species concentrations (N_2O, CO, and CO_2), were made in samples collected from a rocket-borne cryogenic whole air sampler. A large mass-independent isotopic anomaly was observed in CO_2, which may in part derive from photochemical coupling to ozone (O_3). The data also require an additional isotopic fractionation process, which is presently unidentified. Mesospheric O_2 isotope ratios differed from those in the troposphere and stratosphere. The cause of this isotopic variation in O_2 is presently unknown. The inability to account for these observations represents a fundamental gap in the understanding of the O_2 chemistry in the stratosphere and mesosphere.

The measurement of stable isotope ratios of atmospheric species provides a powerful method for investigating chemical transformation mechanisms in the atmosphere. A particularly important example is stratospheric O_3, for which an ^{18}O enrichment of up to 40% in the $^{18}O/^{16}O$ ratio has been observed (*1–4*). In laboratory studies of isotopic fractionation during O_3 formation, O_3 was produced that was enriched in the heavy isotopes, with $\delta^{17}O = \delta^{18}O$, rather than $\delta^{17}O = 0.5\ \delta^{18}O$ (*5, 6*). The isotope ratios were thus distributed in a mass-independent manner; in a mass-dependent process, the $\delta^{18}O$ variation would be twice that of $\delta^{17}O$ because the relative mass difference is doubled (*5*). It has been demonstrated that the anomalous fractionation occurred in the $O + O_2$ recombination step and was mediated by molecular symmetry factors (*7*). Many of the observed stratospheric O_3 ^{18}O enrichments are significantly greater than those observed in laboratory experiments, which are at most 150 per mil (*8–10*). To date, there is no consistent explanation for this large discrepancy or for the observed variability of the ^{18}O enrichment in stratospheric O_3. The inability to account for these observations represents a fundamental gap in the understanding of stratospheric O_3 chemistry.

Stratospheric CO_2 has also been shown to be enriched in ^{18}O in comparison with tropospheric CO_2 (*11–13*), and it has been shown that stratospheric O_2 isotopes are mass-fractionated independently (*12*). It has been proposed that the CO_2 enrichment may arise from isotopic exchange between CO_2 and $O(^1D)$, with $O(^1D)$ derived from O_3 photolysis (*14*). Laboratory experiments demonstrated that isotopic exchange between $O(^1D)$ and CO_2 produces a mass-independent fractionation, with equal enrichment in the heavy isotopes in CO_2 (*15*). Recent simultaneous $\delta^{17}O$ and $\delta^{18}O$ measurements of stratospheric CO_2 have demonstrated that the magnitude of the mass-independent isotopic anomaly linearly correlates with ^{14}CO activity, which confirms the stratospheric origin of the isotopic enrichment (*13*). The use of simultaneous isotope ratio measurements ($\delta^{17}O$ and $\delta^{18}O$) thus offers an insight into atmospheric chemical processes that cannot be obtained from concentration or measurements of single ($\delta^{18}O$) isotope ratios.

The observation of photochemical coupling between stratospheric O_3 and CO_2 has several implications. First, the CO_2 isotopic measurements provide another probe of the overall oxidation processes of the upper atmosphere (*13*). In particular, estimates of the $O(^1D)$ density can be obtained, which determines the lifetime of some of the more long-lived species, such as N_2O, and is an integral component of the radiative budget of the upper atmosphere. Second, the O_2 isotopes provide another measure of stratosphere-troposphere mixing.

Here, we report the simultaneous measurement of the $\delta^{17}O$ and $\delta^{18}O$ composition of CO_2 and O_2 and the concentrations of N_2O, CH_4, and CO from samples taken in the altitude range of 30 to 60 km. Samples were taken with the use of the rocket-borne cryogenic whole air sampler (CWAS) described by Erdman and Zipf (*16*). The system uses closed-cycle refrigerators to chill 1.8-kg, gold-plated blocks to approximately 15 K. Pneumatically actuated valves open and close at predetermined times to collect whole air samples, with altitudes and sampling column lengths (~1.1 km) determined by radar. The payload is launched by a two-stage Nike-Orion rocket. The two sampling missions reported here (March and May 1992, with two launches for each mission) were launched from the White Sands Missile Range (WSMR), New Mexico (32.4°N, 253.7°E), with three samples collected per flight (Table 1). The altitudes of the samples, the sampling interval, and the absolute sample sizes were nearly iden-

M. H. Thiemens and T. Jackson, Department of Chemistry 0356, University of California at San Diego, La Jolla, CA 92093, USA.
E. C. Zipf, P. W. Erdman, C. van Egmond, Department of Physics and Astronomy, University of Pittsburgh, Pittsburgh, PA 15260, USA.

*To whom correspondence should be addressed.

tical for the flights, which shows the reproducibility of the measurements. To ensure quantitative collection, we measured the amount of air within the samplers and compared it to that expected for a sampling interval. The quantity of air collected matched that expected for the sampling profile within ±5%.

Here, the CO_2 was cryogenically separated from the whole air samples. For O_2 isotopic analysis, the CO_2 was quantitatively converted to O_2 to permit $\delta^{18}O$ and $\delta^{17}O$ measurements. The CO_2 was reacted with BrF_5 in a Ni tube at 800°C for 48 hours (*17*). Isotope measurements were made in a mass spectrometer (Finnigan MAT 251). Whole air aliquots were taken for separation and isotopic analysis of O_2 as described (*18*).

The isotopic data (Fig. 1) were all fractionated mass-independently—that is, $\delta^{17}O \neq 0.5\ \delta^{18}O$. The mass-independent isotopic composition was of the same magnitude as that reported in (*12*) for stratospheric samples collected by balloon flight. There is a clear relation between the isotopic data and trace species concentration profiles (Fig. 2). Concerning the relative behavior of $\delta^{18}O$ versus CH_4 and N_2O concentrations with altitude, at 35 and 40 km for the flights in March and May, a peak in the $\delta^{18}O$ profile was observed. Methane and N_2O possess a similar structure, and this was attributed to the transport of stratospheric air derived from equatorial latitudes (*19*). The quasi-mirror image behavior for both data sets may arise from the involvement of $O(^1D)$; elevated $O(^1D)$ levels increase the $\delta^{18}O$ in CO_2 while simultaneously lowering the N_2O and CH_4 concentrations because reaction with $O(^1D)$ is their dominant sink (*20*). Such enhanced levels of $O(^1D)$ require a stratospheric source for the transported air parcel. The height of the observed fold is apparently seasonal, with the winter peak occurring at higher altitudes than that for spring. This variation may reflect stratospheric and mesospheric circulation dynamics, given that meridional transport differs between winter and summer (*21*).

The interaction between $O(^1D)$ and CO_2 is consistent with the laboratory data of Wen and Thiemens (*15*), who showed that the production of the short-lived CO_3* transition state, intermediate in the isotopic exchange between CO_2 and $O(^1D)$, produces a mass-independent isotopic composition in CO_2, with equal ^{17}O and ^{18}O enrichments in CO_2. Enhanced values of $\delta^{18}O$ in CO_2 derive from higher number densities of atomic O, longer interaction times, or both. The anti-correlation between the atmospheric ^{18}O enrichment and the N_2O and CH_4 mixing ratios reflects increased O_3 photolysis, the source of $O(^1D)$. The critical proof is the observation of the mass-independent isotopic composition.

At 55 km (27 May flight), a peak in $\delta^{18}O$ exists but without an accompanying CH_4 inflection. This suggests that the mesosphere may be a contributor to the O_2 isotopic composition of stratospheric CO_2, because of larger amounts of atomic O and smaller amounts of CH_4. Injection of mesospheric air would thus be detectable from the O_2 isotopic signature but not from the CH_4 concentration. The CO altitudinal data also suggest inputs of mesospheric air. For both sampling missions, an increase in the CO mixing ratio above 40 km was observed, which indicates a mesospheric source. Carbon monoxide in this altitudinal region primarily comes from mesospheric CO_2 photolysis (*22*). The lack of a corresponding dip in the N_2O and CH_4 data and their suppressed concentrations with respect to the measurements in March also suggest the injection of upper level air rich in $O(^1D)$ and CO and depleted in CH_4 and N_2O.

Another important feature associated with the CO_2 isotopic data in Fig. 1 is that the data define a straight line with a slope nearly 1.0. If the isotopic composition were a result only of the process of isotopic exchange with $O(^1D)$, the best-fit line should have a slope = 1.0 and pass through the isotopic composition of tropospheric CO_2 ($\delta^{18}O \approx 40$ per mil, $\delta^{17}O \approx 20$ per mil). The observed best-fit line of the stratospheric CO_2 isotopic data does not intersect the terrestrial fractionation line at the tropospheric value but rather at a value for $\delta^{18}O$ of approximately 34 per mil. These observations require an additional process, along with exchange between $O(^1D)$ and CO_2. It has been shown (*15*) that isotopic exchange between $O(^1D)$ and CO_2 defines a $\delta^{17}O = \delta^{18}O$ fractionation line passing through the bulk CO_2 reservoir.

The expected isotopic fractionation line (Fig. 1) would arise if $O(^1D)$ exchanged with CO_2 of approximate tropospheric isotopic composition (CO_2 at 1300 m at White Sands has an isotopic composition of $\delta^{18}O$ of 41.5 per mil). The data clearly do not pass through the $\delta^{18}O$ value of tropo-

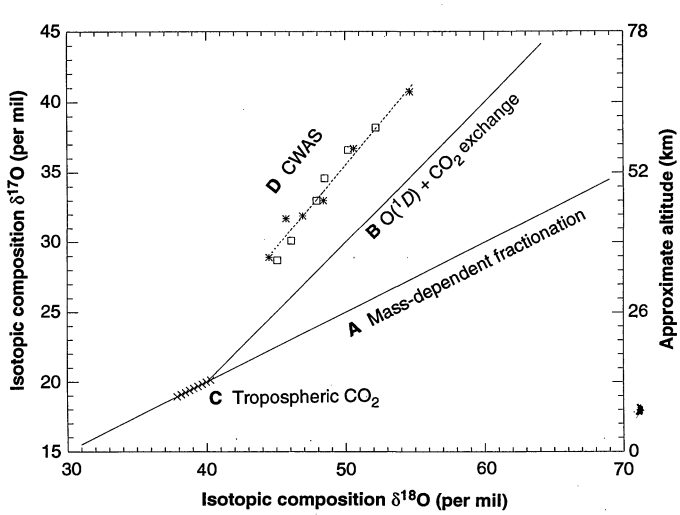

Fig. 1. A three-isotope plot showing the O_2 isotopic composition of atmospheric CO_2 for different fractionation processes. Line **A** represents the bulk terrestrial mass fractionation line, whereas line **B** results from additional isotopic exchange between tropospheric CO_2 and $O(^1D)$. Line **C** represents the measured range of tropospheric CO_2 isotopes (*12*). Line **D** is the best-fit line for the O_2 isotopic composition of the upper atmospheric CO_2 samples measured here; asterisks represent the March, and squares the May, data. The data define a line of slope 1.16, with a linear regression constant of 0.98. The offset of line D from line B is the result of a secondary fractionation process, the source of which is at present unknown.

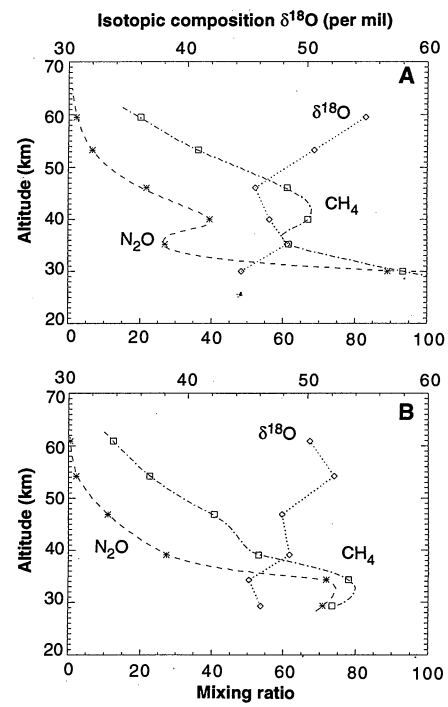

Fig. 2. $\delta^{18}O$ profiles for CO_2 and O_2 isotopic composition and CH_4 and N_2O mixing ratio profiles for samples taken on (**A**) 12 and 15 March 1992 and (**B**) 22 and 27 May 1992. The mixing ratios for N_2O and CH_4 are in parts per billion and parts per billion/10, respectively. Note the anti-correlation between the ^{18}O enrichment and the N_2O and CH_4 mixing ratios, which is indicative of increased O_3 photolysis, the source of $O(^1D)$.

spheric CO_2 and require a second fractionation process that offsets the observed data. The source of this secondary fractionation process observed in the stratospheric and mesospheric samples is not known. Our CO observations along with the increasing magnitude of isotopic fractionation suggest a mesospheric origin for the fractionation. Stratospheric concentrations of $O(^1D)$ peak at an altitude of approximately 48 km with a number density of 200 to 300 cm^{-3} (*23*). The $O(^1D)$ concentrations rise rapidly by more than an order of magnitude in the mesosphere. The significantly enhanced levels of electronically excited atomic O would produce greater ^{17}O,^{18}O enrichments, which is consistent with our observations. The stratospheric isotopic CO_2 data reported by Thiemens *et al.* (*12*) agree with the data presented here, with the highest altitude samples (~35 km) lying along the fractionation line D (Fig. 1), whereas the lower altitude samples lie on a line with a slope of ~1 passing through tropospheric CO_2 values. Thus, the higher altitude samples appear to possess the greatest heavy isotope enrichment. Sampling artifacts can be ruled out as the CO_2 concentration for all altitudes was 350 ppm (parts per million), the amount expected if all the expected CO_2 was recovered.

It is not known what additional processes might occur in the mesosphere. For example, the effect of temperature on the exchange process is not known for the relevant in situ temperatures. The effect of ion-molecule reactions, for example, charge transfer, on isotopic composition is also unknown. Resolution of the source of this isotopic component is of importance as the magnitude of the anomalous component is sufficiently large that the absolute amount of energy required to produce the observed anomalous isotopic composition represents an important process in the upper atmosphere.

The molecular O_2 isotopic data also provided further evidence for mesospheric input into the stratosphere of isotopically distinctive components. All of the data in Table 1 agree with the tropospheric O_2 value, $\delta^{18}O = 23.5$ (*24*), within the error limit of ±0.1 per mil; the only exceptions to this are the two uppermost March samples ($\delta^{18}O = 23.1$ per mil), which differ by 0.4 per mil, significantly beyond error limits. This is the first observation of a variation in the O_2 isotopic composition of atmospheric O_2. In hundreds of tropospheric measurements of air samples taken in the United States, Australia, and Europe, the value has been constant to within ±0.04 per mil; thus, the mesospheric variation observed here is significant.

It has been suggested that an upper atmospheric process could alter the O_2 isotopes on the basis of the measured O_2 isotopic composition of extraterrestrial Fe spherules, which acquire their O_2 at altitudes above ~100 km (*25*). It was suggested that a source of heavy O ($\delta^{18}O > 40$ per mil) at this altitude may exist, and a qualitative model, based on calculations by Colegrove *et al.* (*26*), was provided. Because of the dominance of O_2 photolysis over recombination at altitudes above 80 km, there is a net downward flux of O atoms and upward flux of O_2 molecules (*26*). During such motion in the atmosphere, the model predicts that the associated isotopic fractionation for O atoms is greater than that for O molecules because of the smaller mass of the former. The net result could be the creation of an isotopic composition with heavy isotope enrichment in the upper levels and light isotope (total O) enrichment in the lower levels (*25*). The lower level (light isotopes) of this circulation cell would be the upper mesosphere, which could serve as a source of the isotopically light O_2 measured in the March flight. Although later measurement of the Fe isotopes in similar Fe spherules showed that the ^{18}O enrichment derives from atmospheric evaporation effects (*27*), it is possible that some component of the features suggested in (*25*) is qualitatively correct. At present, no source of the isotopic fractionation process in O_2 can be specified conclusively; however, the CO_2 and O_2 isotopic data tentatively suggest that the source region is the upper mesosphere, particularly because the molecular O_2 isotopic fractionation was observed in winter, when the net air mass trajectory is downward from the upper mesosphere (*21*).

Carbon dioxide photolysis may be considered a possible contributing factor to the observed CO_2 isotopic composition. It is known that at altitudes above 55 km, the primary CO source is photodissociation of CO_2 (*22*), consistent with our data here, which show increasing CO concentrations with increasing altitude. It is known that in O_3 photolysis the lighter isotopes are preferentially dissociated because of their higher relative vibrational frequency in a nearly mass-dependent fashion (*28*). If the same were true for CO_2, the residual CO_2 would be isotopically heavy; however, our observations suggest that a light component is required. Photolysis would thus shift the data in the wrong direction. In addition, the measured CO_2/CO ratio at 59.5 km in the March flight was 2784; if all CO were derived from CO_2 photolysis, this CO_2/CO ratio would be too large to alter the CO_2 isotopic composition for any reasonable single-stage fractionation factor associated with CO_2 photolysis. The requirements are particularly forbidding at 30.0 km (March), where the CO_2/CO ratio is ~14,000; thus, our observations cannot be attributed purely to CO_2 photolysis effects. It is unclear at present what process, along with $O(^1D) + CO_2$ isotopic exchange, is responsible for the observed CO_2 isotopic data. The magnitude of the isotopic fractionation is large, and the process represents an important reaction in upper atmospheric chemistry.

Our results from the isotopic and trace species concentration data in whole air samples collected from flights of the rocket-borne CWAS clearly show that combined isotope and trace species measurements provide a wealth of data that reflect both upper atmospheric chemical interactions and circulation dynamics. The isotope data reveal dynamic features that could not be obtained from only concentration or measurement of the ratios of single isotopes. Presently unexplained isotopic anomalies reside in both molecular O_2 and CO_2. In addition, there

Table 1. Flight isotopic and trace species concentration data for the rocket-borne whole air cryogenic sampler. Isotopic compositions are reported with respect to standard mean ocean water (SMOW).

Date	Altitude (km)	Isotopic composition*						CO (ppbv)	CO_2* (ppm)
		CO_2		O_2		N_2O (ppbv)	CH_4 (ppbv)		
		$\delta^{18}O$	$\delta^{17}O$	$\delta^{18}O$	$\delta^{17}O$				
				March 1992					
15	30.0	44.5	28.9	23.6	12.2	89.1 ± 2.4	933 ± 30	25.0 ± 3	350.2
15	35.2	48.4	33.0	23.4	12.0	27.0 ± 1.0	617 ± 20	40.5 ± 3	350.5
15	40.0	46.9	31.9	23.6	12.0	39.5 ± 1.2	670 ± 22	31.9 ± 3	350.2
12	46.1	45.7	31.7	23.4	12.0	21.8 ± 0.9	613 ± 20	56.1 ± 3	350.5
12	53.3	50.6	36.7	23.1	11.8	6.7 ± 0.5	363 ± 13	81.8 ± 3	350.3
12	59.5	54.9	40.5	23.1	11.8	2.2 ± 0.2	200 ± 9	126 ± 3	350.8
				May 1992					
22	29.3	46.1	30.1	23.5	11.8	70.8 ± 2.1	734 ± 24	25 ± 3	353.7
22	34.3	45.1	28.7	23.5	11.8	71.8 ± 2.1	780 ± 25	22 ± 3	353.6
22	39.1	48.5	34.6	23.4	11.8	27.2 ± 1.0	530 ± 18	18 ± 3	353.7
27	46.9	47.9	33.0	23.4	11.8	11.0 ± 0.5	406 ± 14	18 ± 3	353.4
27	54.2	52.2	38.2	23.5	11.8	2.2 ± 0.2	225 ± 10	44 ± 3	353.4
27	60.9	50.2	36.6	23.4	11.8	1.0 ± 0.2	125 ± 6	82 ± 3	353.4

*Uncertainties are approximately ±0.2 ppmv (2σ error bars)

are seasonal features observed in both the trace species and isotopic altitudinal profiles. Further measurements may define both the source of the anomalous fractionations and the seasonal character.

REFERENCES AND NOTES

1. K. Mauersberger, *Geophys. Res. Lett.* **8**, 935 (1981).
2. M. M. Abbas *et al.*, *J. Geophys. Res.* **92**, 13239 (1989).
3. A. Goldman *et al.*, *ibid.* **94**, 8467 (1989).
4. B. Schueler, J. Morton, K. Mauersberger, *Geophys. Res. Lett.* **17**, 1295 (1990).
5. M. H. Thiemens and J. E. Heidenreich III, *Science* **219**, 1073 (1983).
6. The δ notation is defined as follows: $\delta^{18}O = (R^{18}/R^{18}_{std} - 1)\ 1000$; $\delta^{17}O = (R^{17}/R^{17}_{std} - 1)\ 1000$. The subscript "std" refers to the conventional standard, which for O is standard mean ocean water (SMOW). R^{18} is the $^{18}O/^{16}O$ ratio, and R^{17} is the $^{17}O/^{16}O$ ratio.
7. J. E Heidenreich III and M. H. Thiemens, *J. Chem. Phys.* **84**, 2129 (1986).
8. M. H. Thiemens and T. Jackson, *Geophys. Res. Lett.* **15**, 639 (1988).
9. J. J. Morton *et al.*, *J. Geophys. Res.* **95**, 901 (1990).
10. S. M. Anderson *et al.*, in *Isotope Effects in Gas Phase Chemistry*, J. A. Kaye, Ed. (American Chemical Society, Washington, DC, 1992), pp. 156–166; M. H. Thiemens, *ibid.*, pp. 138–154.
11. T. Gamo *et al.*, *Tellus* **41B**, 127 (1989).
12. M. H. Thiemens, T. Jackson, K. Mauersberger, B. Schueler, J. Morton, *Geophys. Res. Lett.* **18**, 669 (1991).
13. M. H. Thiemens, T. L. Jackson, C. A. M. Brenninkmeijer, *ibid.* **22**, 255 (1995).
14. Y. L. Yung, W. B. Demore, J. P. Pinto, *ibid.* **18**, 13 (1991).
15. J. S. Wen and M. H. Thiemens, *J. Geophys. Res.* **98**, 12801 (1993).
16. P. Erdman and E. Zipf, *Rev. Sci. Instrum.* **53**, 106 (1982).
17. S. K. Bhattacharya and M. H. Thiemens, *Z. Naturforsch.* **44a**, 435 (1989).
18. M. H. Thiemens and D. Meagher, *Anal. Chem.* **56**, 201 (1984). The error associated with cryogenic separation of CO_2, fluorination, purification, and mass spectrometric analysis, based on replicated tropospheric CO_2 analysis and standard CO_2 conversion and measurement, is approximately ±0.1 per mil for both $\delta^{17}O$ and $\delta^{18}O$. On the basis of analysis of several hundred tropospheric separations and analysis, for O_2 the error is ±0.04 per mil for $\delta^{18}O$ and 0.08 per mil for $\delta^{17}O$. The amount of O_2 measured from the different flights was identical; thus, the error is assumed to be the same.
19. M. R. Gunsun *et al.*, *J. Geophys. Res.* **95**, 13867 (1990).
20. E. B. Burnett and C. R. Burnett, *J. Atmos. Chem.* **21**, 13 (1995).
21. G. Brasseur and S. Solomon, *Aeronomy of the Middle Atmosphere* (Reidel, Dondrecht, 1984), pp. 32–82.
22. M. Allen, Y. Y. Yung, J. W. Waters, *J. Geophys. Res.* **86**, 3617 (1981).
23. P. M. Banks and G. Kockarts, *Aeronomy, Part A* (Academic Press, New York, 1973).
24. P. Kroopnick and H. Craig, *Science* **175**, 54 (1972).
25. R. N. Clayton, T. K. Mayeda, D. E. Brownlee, *Earth Planet. Sci. Lett.* **79**, 235 (1986).
26. F. D. Colegrove *et al.*, *J. Geophys. Res.* **70**, 4931 (1965).
27. A. M. Davis *et al.*, *Lunar Planet. Sci.* **XXII**, 281 (1991).
28. S. K. Bhattacharya and M. H. Thiemens, *Geophys. Res. Lett.* **15**, 9 (1988).

29. We gratefully acknowledge NSF (grant ATM-9321202) and the National Aeronautics and Space Administration (grant NAG 5-609) for support.

22 June 1995; accepted 8 September 1995

Logic Gates Made from Polymer Transistors and Their Use in Ring Oscillators

A. R. Brown,* A. Pomp, C. M. Hart, D. M. de Leeuw

Metal-insulator-semiconductor field-effect transistors have been fabricated from polymer semiconductors that can be processed from solution. The performance of these transistors is sufficient to allow the construction of simple logic gates that display voltage amplification. Successful coupling of these gates into ring oscillators demonstrates that these logic gates can switch subsequent gates and perform logic operations. The ability to perform logic operations is an essential requirement for the use of polymer-based transistors in low-cost low-end data storage applications.

One major application for polymeric metal-insulator-semiconductor field-effect transistors (MISFETs) (*1–4*) is in low-end data storage, such as chip cards and identification tags. Here the use of crystalline silicon technology is inappropriate: The excellent electrical performance of silicon, in terms of switching speed and small volume, is not required, and the bonding of silicon chips onto flexible plastic substrates dominates costs. The component parts of a MISFET are an insulator layer, conducting contacts, and a semiconductor layer. Soluble organic insulators are well known [such as poly(methyl methacrylate) and poly(vinyl chloride)], and recently Garnier *et al.* (*2*) have demonstrated that conducting contacts for such polymer MISFETs can be achieved by printing techniques. If a solution-processible organic semiconductor is also used, low-cost large-area electronics for data storage can be realized by using only printing processing steps directly onto plastic substrates (rendering expensive photolithographic steps obsolete and avoiding incompatibility problems).

However, electronic circuits with a polymer as the active semiconductor have not been reported. Until now, polymer MISFETs have not been able to display voltage amplification, which is a fundamental requirement for the construction of useful logic gates. Only if the logic gates can switch subsequent gates does integration become possible. We report here on the successful construction of polymer MISFETs that do display voltage amplification. Two different solution-processible organic semiconductors were used. The MISFETs have been used to fabricate both inverter and NOR gates. Switching of one gate by another is demonstrated in ring oscillators constructed from five identical coupled stages.

These gates have been realized with the use of precursor-route through-conjugated polymers. Through-conjugated polymers are intractable, being neither soluble nor fusible. Solution processibility has been successfully introduced to conjugated polymers such as polythiophenes and poly(paraphenylenes) by the introduction of solubilizing side chains (for example, alkyl and alkoxy groups). However, these side chains have a detrimental effect on the charge-carrier mobility because they both decrease through-conjugation (*1*) and decrease π-π overlap of neighboring chains (*5*). In a precursor route, solubilizing side chains are chosen that can be eliminated later to leave only the through-conjugated polymer. Hence, precursor polymers are particularly suited to be the active semiconductor in polymeric MISFETs, combining solution processibility with good electrical properties (*6*). Here we use oligomeric pentacene and fully polymeric poly(thienylenevinylene) (PTV),

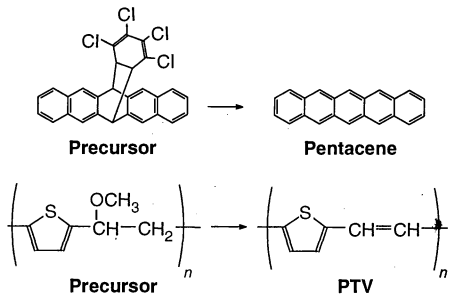

Fig. 1. Chemical structures of pentacene, PTV, and their precursors. Both elimination reactions occur at 140°C for 1 hour; pentacene is realized in vacuo and PTV in N_2 and HCl.

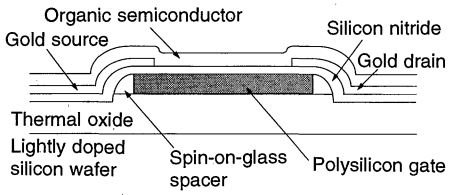

Fig. 2. Schematic cross section of transistors used in this study.

Philips Research Laboratories, Professor Holstlaan 4, 5656 AA Eindhoven, Netherlands.

*To whom correspondence should be addressed.